Leakage loss and bandgap analysis in air-core photonic bandgap fiber for nonsilica glasses

Jonathan Hu and Curtis R. Menyuk

University of Maryland Baltimore County,
5200 Westland Blvd., Baltimore, MD 21227
hu1@umbc.edu

http://www.umbc.edu/photonics

Abstract: We calculate the minimum leakage loss and maximum relative bandgap as a function of the air-filling factor in a photonic bandgap fiber for a refractive index between 1.4 and 2.8. We analyze the mode properties for two maxima of the relative bandgap when we vary the air-filling factor and the refractive index. The maximum relative bandgap accurately predicts the optimal operating air-filling factor corresponding to lowest leakage loss.

OCIS codes: (060.2280) Fiber design and fabrication; (060.2400) Fiber properties; (060.2390) Fiber optics, infrared

References and links

1. J. C. Knight, J. Broeng, T. A. Birks, and P. St. J. Russell, "Photonic band gap guidance in optical fibers," Science, **282**, 1476–1478 (1998).
2. J. Broeng, S. E. Barkou, T. Søndergaard, A. Bjarklev, "Analysis of air-guiding photonic bandgap fibers," Opt. Lett. **25**, 96–98 (2000).
3. K. Saitoh and M. Koshiba, "Leakage loss and group velocity dispersion in air-core photonic bandgap fibers," Opt. Express **11**, 3100–3109 (2003), http://www.opticsexpress.org/abstract.cfm?URI=OPEX-11-23-3100.
4. B. Kuhlmey, R. McPhedran, C. de Sterke, P. Robinson, G. Renversez, and D. Maystre, "Microstructured optical fibers: where's the edge?," Opt. Express **10**, 1285–1290 (2002), http://www.opticsinfobase.org/abstract.cfm?URI=oe-10-22-1285.
5. J. M. Pottage, D. M. Bird, T. D. Hedley, T. A. Birks, J. C. Knight, P. St.J. Russell and P. J. Roberts, "Robust photonic band gaps for hollow core guidance in PCF made from high index glass," Opt. Express **11**, 2854–2861 (2003), http://www.opticsexpress.org/abstract.cfm?URI=OPEX-11-22-2854.
6. T. M. Monro, Y. D. West, D. W. Hewak, N. G. R. Broderick, and D. J. Richardson, "Chalcogenide holey fibres," Electron. Lett. **36**, 1998–2000 (2000).
7. L. B. Shaw, J. S. Sanghera, and I. D. Aggarwal, "As-S and As-Se based photonic band gap fiber for IR laser transmission," Opt. Express **11**, 3455–3460 (2003), http://www.opticsexpress.org/abstract.cfm?URI=OPEX-11-25-3455.
8. S. G. Johnson, and J. D. Joannopoulos, "Block-iterative frequency-domain methods for Maxwell's equations in planewave basis," Opt. Express **8**, 173–190 (2001), http://www.opticsexpress.org/abstract.cfm?URI=OPEX-8-3-173.
9. X. Feng, A. K. Mairaj, D. W. Hewak, and T. M. Monro, "Nonsilica glasses for holey fibers," J. Lightwave Technol. **23**, 2046–2054 (2005).
10. J. D. Joannopoulos, R. D. Meade, and J. N. Winn, *Photonic Crystals*, (Princeton University Press, 1995).
11. T. P. White, B. T. Kuhlmey, R. C. McPhedran, D. Maystre, G. Renversez, C. M. de Sterke, and L. C. Botten, "Multipole method for microstructured optical fibers. I. Formulation," J. Opt. Soc. Am. B **19**, 2322–2330 (2002).
12. B. T. Kuhlmey, T. P. White, G. Renversez, D. Maystre, L. C. Botten, C. M. de Sterke, R. C. McPhedran, "Multipole method for microstructured optical fibers. II. Implementation and results," J. Opt. Soc. Am. B **19**, 2331–2340 (2002).

#75986 - $15.00 USD Received 13 October 2006; revised 21 December 2006; accepted 22 December 2006

13. H. K. Kim, M. J. F. Digonnet, G. S. Kino, J. Shin, and S. Fan, "Simulations of the effect of the core ring on surface and air-core modes in photonic bandgap fibers," Opt. Express **12**, 3436–3442 (2004), http://www.opticsexpress.org/abstract.cfm?URI=OPEX-12-15-3436.
14. G. J. Pearce, J. M. Pottage, D. M. Bird, P. J. Roberts, J. C. Knight, and P. S. Russell, "Hollow-core PCF for guidance in the mid to far infra-red," Opt. Express **13**, 6937–6946 (2005), http://www.opticsexpress.org/abstract.cfm?URI=OPEX-13-18-6937.
15. J. West, C. Smith, N. Borrelli, D. Allan, and K. Koch, "Surface modes in air-core photonic band-gap fibers," Opt. Express **12**, 1485–1496 (2004), http://www.opticsinfobase.org/abstract.cfm?URI=oe-12-8-1485.

1. Introduction

Air-core photonic bandgap fibers (PBGFs), in contrast to some other types of holey fiber, guide light through the photonic bandgap effect, instead of using total internal reflection [1, 2]. PBGFs have the potential to provide very low-loss transmission, along with delivery of high power and low nonlinearity. Due to the finite number of air hole rings, the modes in the air-core PBGFs are leaky modes. There are several commonly used ways to measure the extent to which air holes fill the fiber cladding. The air-filling factor, which is commonly used for a fiber with circular holes, is defined as the ratio of the hole diameter to the pitch, d/Λ [3, 4]. Pitch is defined as the distance between the centers of the nearby holes. Reference 5 uses both half the air-filling factor, which it refers to as r_{hole}/Λ, and it also uses the air-filling fraction. The air-filling fraction is defined as the ratio of the air to the glass area in a unit cell. The air-filling fraction is related to the air-filling factor by the relationship $(\sqrt{3}\pi/6)(d/\Lambda)^2$. We report results here as a function of both the air-filling factor and the air-filling fraction. Research on silica fiber shows that a larger air-filling factor in air-core PBGFs leads to wider bandgaps and hence better mode confinement [3]. Pottage, *et al.* suggest using lower air-filling factors to obtain a wider bandgap for high-index glass [5]. The assumption is that a wider relative bandgap leads to lower leakage loss. However, the loss due to mode leakage in high-index glass with lower air-filling factors has not been previously calculated, and this assumption remains unverified. In this paper, we calculate the relative bandgap when we vary the air-filling factor and the refractive index. The relative bandgap has two maxima in a two-dimensional contour plot as a function of the air-filling factor and the refractive index. With a refractive index of 2.4, which is close to the refractive index of chalcogenide fiber at $\lambda = 4\ \mu$m [6, 7], there is an optimal air-filling factor at about 0.8 that minimizes the loss. Also, we show that the air-filling factors for the minimum loss and maximum relative bandgap coincide for a wide range of refractive indices. Thus the simple unit-cell plane-wave analysis, although it cannot be used to calculate the leakage loss, correctly predicts the optimal operating air-filling factor of air-core PBGFs in the cases that we studied, as Pottage, *et al.* suggested [5]. Although the material loss is not included in the simulation, the analysis of leakage loss indicates the minimum possible loss for the PBGF design.

2. Bandgap and mode analysis

In the plane-wave analysis, one assumes a periodic structure, so that this analysis cannot be used to calculate the loss due to leakage. We use the full-vectorial plane-wave method to obtain the bandgap in a two-dimensional photonic crystal cladding arranged in a triangular pattern [8]. We used a grid resolution of $\Lambda/128$ and verified that the difference between these results and the results with a grid resolution of $\Lambda/64$ differ by less than 1%. Figures 1(a) and (b) show the calculated bandgap diagrams for a refractive index of 1.45 with an air-filling factor of 0.9 and a refractive index of 2.4 with an air-filling factor of 0.8, respectively. We note that the normalized frequency $\omega\Lambda/2\pi c$ shown on the ordinate is also equal to the pitch-wavelength ratio Λ/λ. In these figures, the dashed lines represent the bandgap edges of the photonic crystal

#75986 - $15.00 USD Received 13 October 2006; revised 21 December 2006; accepted 22 December 2006

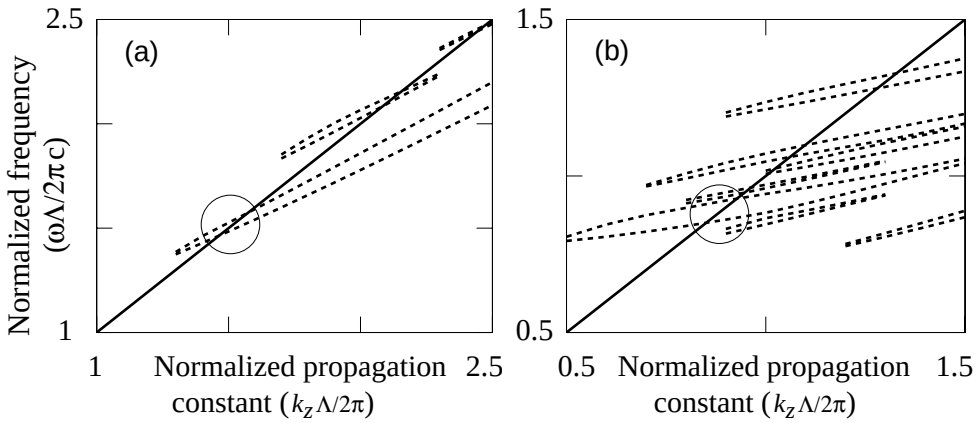

Fig. 1. Bandgap diagrams for (a) a refractive index of 1.45 with an air-filling factor of 0.9 and (b) a refractive index of 2.4 with an air-filling factor of 0.8, respectively. The refractive indices of 1.45 and 2.4 correspond to silica and chalcogenide glass, respectively.

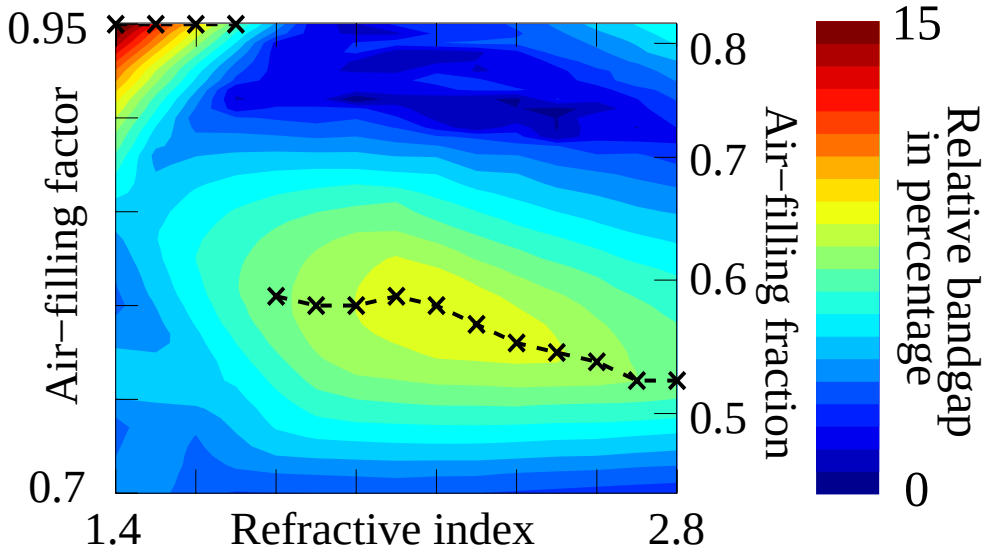

Fig. 2. The contour plot for the maximum relative bandgap as a function of the air-filling factor and the refractive index. The corresponding air-filling fraction is also shown. The black *x*-marks represent the air-filling factors corresponding to the maximum relative bandgap at each refractive index. Two black dashed curves connect *x*-marks in the two relative bandgap maxima in the contour plot. There exists a discontinuity of the maximum relative bandgap around a refractive index of 1.8.

cladding. The solid lines represent the air lines. We found several bandgaps that cross the air line in our range of interest. In order to choose the best bandgap, we define a relative air-crossing bandgap or simply a relative bandgap, as the ratio of the bandgap intersection with the air line to the middle of the bandgap in the air line, which is the same as the normalized gap

#75986 - $15.00 USD Received 13 October 2006; revised 21 December 2006; accepted 22 December 2006

width defined in Ref. 5. This definition takes into account that bandgaps at larger frequencies must open more widely to have losses comparable to bandgaps at lower frequencies. We stress that it is the relative bandgap, not the absolute bandgap, that correlates well with the loss. Shaw, *et al.* showed that with a refractive index of 2.8, one obtains larger absolute bandgaps at $d/\Lambda = 0.996$ [7]. Nevertheless, the relative bandgap is larger when $d/\Lambda = 0.8$, and the loss is lower. We circle the largest relative bandgaps in Figs. 1(a) and (b). In Fig. 2, we show in a contour plot the relative bandgap as a function of the air-filling factor and the refractive index. We choose a maximum refractive index of 2.8 since commercial optical-fiber glasses do not have refractive indices higher than 2.8 [5, 9]. In this figure, the black *x*-marks represent the air-filling factors corresponding to the maximum relative bandgap at each refractive index. Two black dashed curves connect *x*-marks in the two relative bandgap maxima in the contour plot. There exists a discontinuity of the maximum relative bandgap around a refractive index of 1.8. This discontinuity occurs because the bandgap with the maximum relative bandgap changes.

We found that for a refractive index below 1.8, the relative bandgap always increases as the air-filling factor increases when the air-filling factor is larger than 0.9, as shown in Fig. 2. This behavior can be understood by examining the mode structure at the extrema of the bands that surround the largest relative bandgap. Figure 3 shows the band diagram when we use a refractive index of 1.45 and an air-filling factor of 0.92, with a normalized propagation constant equal to $k_z\Lambda/2\pi$ = 1.6. The largest relative bandgap occurs between bands 4 and 5, and the extrema occur at the Γ point. Figures 4(a) and (b) show the normalized magnitude of the Poynting flux in the 4th and 5th bands. Note that most of the flux in the 4th band is located in the spots, which are the large glass regions between three holes in the triangular structure. However, most of the flux in the 5th band is located in the veins, which are the long thin connections between two spots. As the air-filling factor increases and the veins become thinner, the flux in the 4th band remains almost unchanged in the spot, but the flux in the 5th band is pushed into the air. Figure 5 shows the fill factor for the 4th and 5th bands as a function of air-filling factor. Fill factor is an appropriate measure of the degree of concentration of the displacement fields in the glass regions, defined as [10]

$$f = \frac{\int\limits_{\text{glass}} [|\mathbf{D}(x,y)|^2/\varepsilon(x,y)]dxdy}{\int\limits_{\text{all space}} [|\mathbf{D}(x,y)|^2/\varepsilon(x,y)]dxdy}. \tag{1}$$

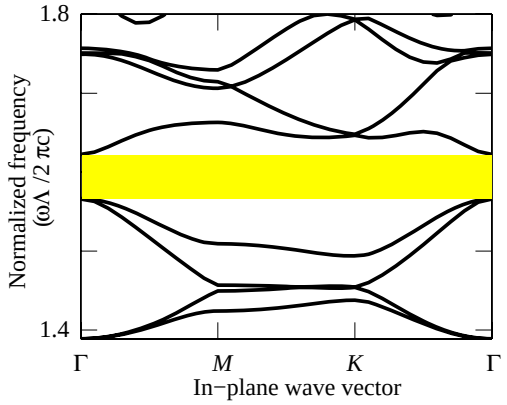

Fig. 3. Band diagram when we use a refractive index of 1.45 and an air-filling factor of 0.92. Yellow indicates the largest relative bandgap.

#75986 - $15.00 USD Received 13 October 2006; revised 21 December 2006; accepted 22 December 2006

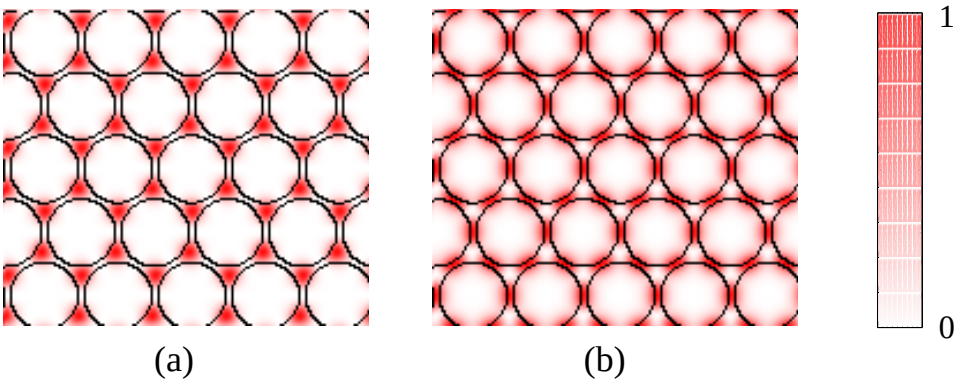

Fig. 4. Magnitude of Poynting flux, normalized to its peak, in the (a) 4th and (b) 5th band. The red regions correspond to a large Poynting flux. Most of the flux in the 4th band is located in the spots, which are the large glass regions between three holes in the triangular structure. However, most of the flux in the 5th band is located in the veins, which are the long thin connections between two spots.

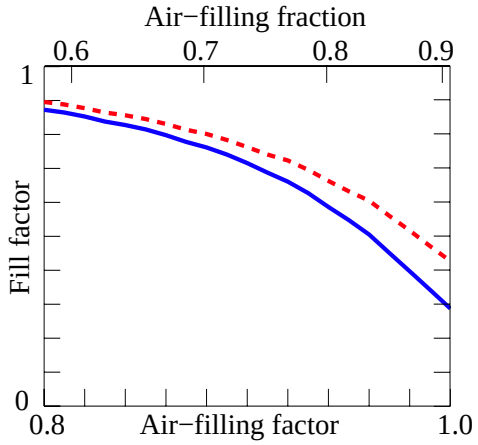

Fig. 5. Fill factor as a function of the air-filling factor. The corresponding air-filling fraction is also shown. Red dashed and blue solid curves represent the fill factor for the 4th and 5th bands, respectively.

Red dashed and blue solid curves in Fig. 5 represent the fill factor for the 4th and 5th bands, respectively. The fill factor for the 5th band decreases faster than the fill factor for the 4th band as the air-filling factor increases. It has been shown that the mode's frequency decreases at a fixed propagation constant k_z when the displacement field **D** is concentrated in the regions of high dielectric constant [10]. Hence, the frequency increase in the 5th band is faster than the increase in the 4th band as the air-filling factor increases, which implies that the bandgap opens wider. This result agrees with the loss analysis in Fig. 9 of Ref. 3, which demonstrated that a higher air-filling factor always yields lower loss when the normalized frequency is optimized using a refractive index of silica, which is 1.45. On the other hand, if we increase the refractive index, the mode's frequency decreases for each k_z and eventually falls below the airline, so that air-guided modes are no longer possible.

#75986 - $15.00 USD Received 13 October 2006; revised 21 December 2006; accepted 22 December 2006

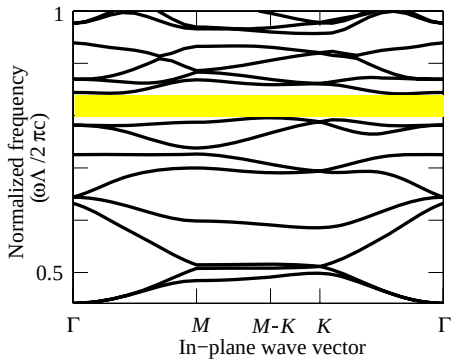

Fig. 6. Band diagram when we use a refractive index of 2.4 and an air-filling factor of 0.75. Yellow indicates the largest relative bandgap.

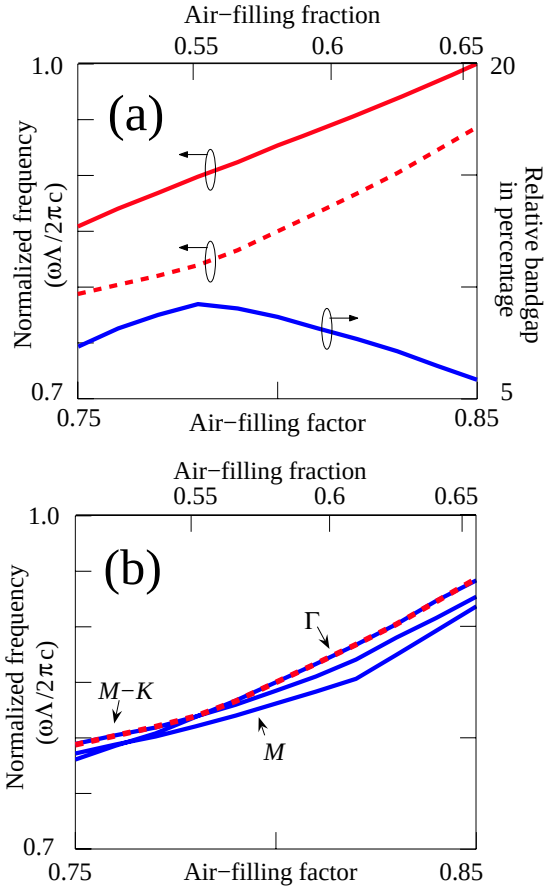

Fig. 7. (a) Red solid and dashed curves represent the lowest frequency in the 9th band and highest frequency in the 8th band as functions of the air-filling factor. (b) The red dashed curve is the same as in (a). Three solid blue curves represent the normalized frequency in the Γ, *M*, and *M*-*K* points as a function of air-filling factor. The corresponding air-filling fraction is also shown.

#75986 - $15.00 USD Received 13 October 2006; revised 21 December 2006; accepted 22 December 2006

By contrast, when the refractive index is above 1.8, the relative bandgap has a maximum at an air-filling factor of about 0.8. To understand this behavior, we show in Fig. 6 the band diagram when we use a refractive index of 2.4 and an air-filling factor of 0.75, with a normalized propagation constant equal to $k_z\Lambda/2\pi$ = 0.8. In this figure, we find that the bandgap between the 8th and 9th bands dominates. Point *M*-*K* is the point where the highest frequency in the 8th band is located. In Fig. 7(a), the red solid and dashed curves represent the lowest frequency in the 9th band and highest frequency in the 8th band as functions of the air-filling factor. At each air-filling factor, the propagation constant is chosen so that the extrema of the 8th and 9th bands cross the air line. Note that the red solid curve is nearly linear, while the red dashed curve is concave. The blue solid curve represents the relative bandgap in percentage, which is the ratio of the difference to the average of the two red curves. Note that blue curve has a maximum at an air-filling factor of 0.78. In Fig. 7(b), the red dashed curve is the same as in Fig. 7(a). Three solid blue curves represent the normalized frequency in the Γ, *M*, and *M*-*K* points as functions of the air-filling factor. The extremum of the 8th band is located at the *M*-*K* point when the air-filling factor is small. As the air-filling factor increases, the frequency at the Γ point increases faster than it does at the *M*-*K* point, and the band extremum shifts to the Γ point when the air-filling factor is between 0.77 and 0.78. As a consequence, the dashed curve is concave. A similar transition occurs when we fix the air-filling factor at 0.8 and vary the refractive index. Hence, the relative maximum bandgap has a maximum that is visible in the center of the Fig. 2. This maximum is less steep than the maximum that is visible in the left upper corner of Fig. 2.

3. Mode leakage loss analysis

Next, we show the leakage loss for this fiber design near the center of the lowest bandgap using the multipole method [11, 12]. In the multipole method, the mode field for each cylindrical hole is expanded in an infinite series of Bessel functions. In numerical analysis, only a finite number

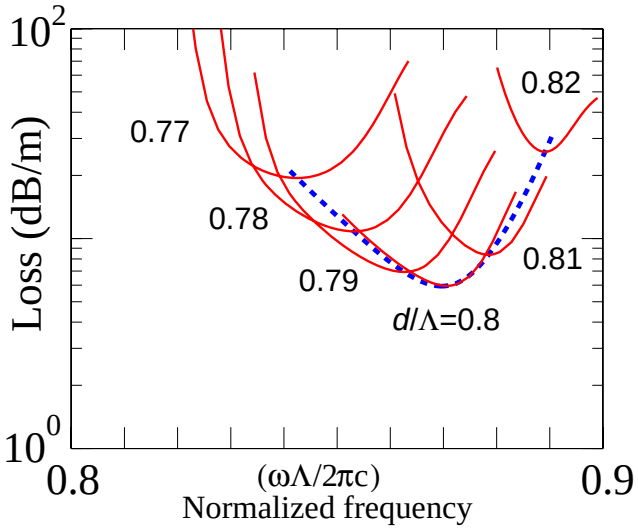

Fig. 8. The leakage loss vs. normalized frequency for air-core PBGFs with 5 air-hole rings, where the air-filling factor is taken as a parameter. The dashed curve represents the loss for the optimized normalized frequency with different air-filling factors (d/Λ). We recall that normalized frequency $\omega\Lambda/2\pi c$ equals the pitch-wavelength ratio Λ/λ. Loss is calculated with a wavelength of 4 μm and a refractive index of 2.4.

#75986 - $15.00 USD Received 13 October 2006; revised 21 December 2006; accepted 22 December 2006

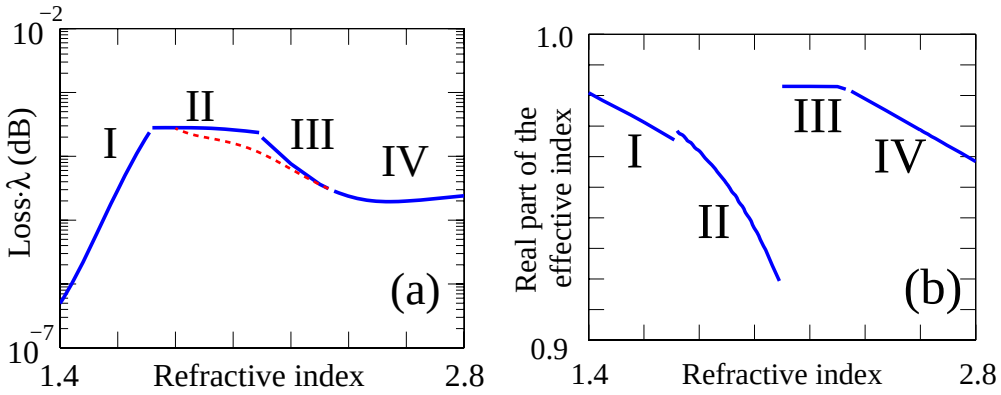

Fig. 9. (a) The normalized leakage loss (loss $\times$ wavelength) as a function of refractive index. (b) The corresponding real part of the effective index.

of Bessel functions may be kept. We denote the maximum order that is kept as $M_{\max}$, and we keep Bessel functions whose order m satisfies $-M_{\max} \leq m \leq M_{\max}$. We used a maximum order $M_{\max} = 6$ in the multipole expansion for the cladding holes and $M_{\max} = 10$ in the multipole expansion for the center hole to obtain n_{eff}, the loss, and the mode intensity, and we verified that using $M_{\max} = 7$ for the cladding holes and 11 for the center hole yields the same n_{eff} to within 0.1% in all the simulations we used in this paper. The variation of the loss is larger, but it is not visible on a logarithmic scale. The glass width between the center air hole and the first layer of air holes is set as small as 0.08Λ in all of our simulations to suppress surface modes [13, 14]. Figure 8 shows the dependence of the normalized frequency of the leakage loss for air-core PBGFs with 5 air-hole rings, where the air-filling factor is taken as a parameter. The red curves in Fig. 8 show that there is a minimum leakage loss for each air-filling factor when one varies normalized frequency. The leakage loss is calculated as $\text{Loss} = 40\pi\text{Im}(n_{\text{eff}})/[\ln(10)\lambda]$, where the $\text{Im}(n_{\text{eff}})$ and λ are the imaginary part of the effective index and the wavelength in meters, respectively [11]. We also plot the loss for optimized normalized frequency with different air-filling factors in this figure as a dashed curve, which connects all the minima of the solid curves. The dashed curves in Fig. 8 show that there is a minimum loss with an air-filling factor of 0.8 and a normalized frequency of 0.87. One must optimize both the air-filling factor and the normalized frequency in order to obtain the minimum loss.

We calculated the minimum loss as a function of the refractive index after we optimized both the air-filling factor and the normalized frequency for a refractive index between 1.4 and 2.8. Figure 9(a) shows the normalized minimum loss as a function of the refractive index. There are four curves in Fig. 9(a). The modes in curve I are located at the bandgap between the 4th and 5th bands. The modes in curves II, III, and IV are located at the bandgap between the 8th and 9th bands. The real part of the effective index is shown in Fig. 9(b). As the real part of the effective index approaches the left-hand side of curve IV, the modes become surface-like. In the range of refractive indices in curve III, the search procedure to find the minimum loss finds the mode at the avoided crossing in the middle of the core mode line. Because we only account for leakage loss, the surface-like mode has a lower loss than the core mode in this case. However, in practice this mode will couple to extended modes and have a high loss [15], so that the calculated low loss is not realistic. In order to avoid finding the surface-like mode in the search procedure, we constrain the modes that come from the search procedure to have 75% or more of its mode power in the central air core. With this constraint, we obtain curve III in Fig. 9(a). The red dashed curve in Fig. 9(a) is the result from the optimization without any constraints.

#75986 - $15.00 USD Received 13 October 2006; revised 21 December 2006; accepted 22 December 2006

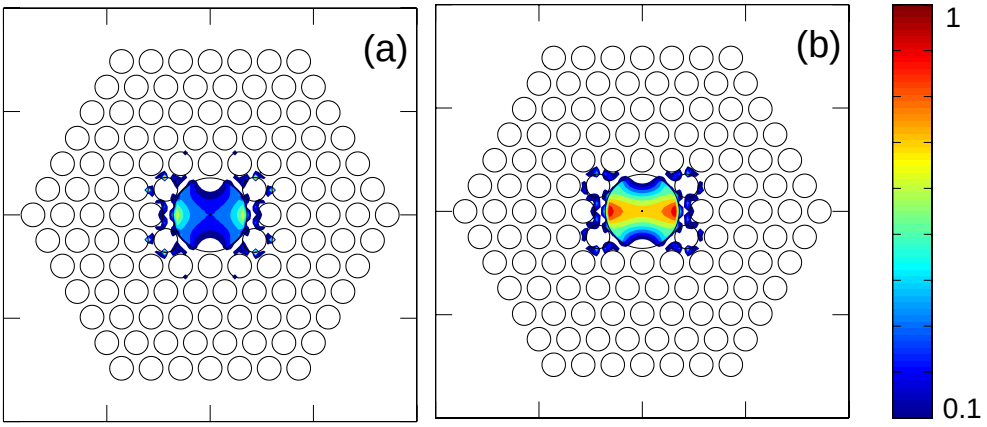

Fig. 10. Geometry and corresponding normalized mode intensity for a 5-layer air-guided PBGF corresponding to (a) the mode found by our optimization procedure without any constraints and (b) the mode found by our optimization procedure with the constraint that more than 75% of the mode power is located in the central air core. Normalized mode intensity smaller than 0.1 is not shown.

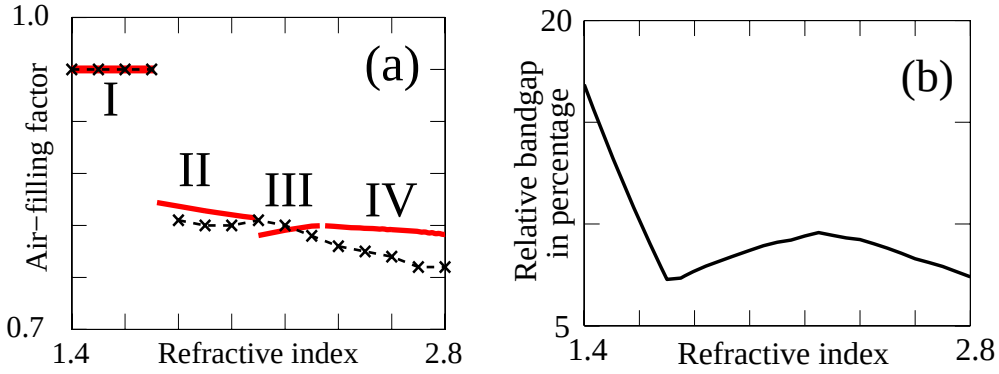

Fig. 11. (a) The solid curves represent the air-filling factor corresponding to minimum loss. The dashed curves with *x*-marks represent the air-filling factor corresponding to the maximum relative bandgap. (b) Relative bandgap when the air-filling factor corresponds to the dashed curve of (a).

Figures 10(a) and (b) show the geometry and the corresponding mode intensity, normalized to its peak, with a refractive index of 2.2 found by the search procedure without any constraints and found by the search procedure with the constraint that more than 75% of the mode power is located in the central air core. In Figs. 10(a) and (b), the black circles represent the hole boundaries and the color contour plots represent the Poynting flux. The leakage losses calculated by the multipole method corresponding to Figs. 10(a) and (b) are 16 and 19 dB/m with a wavelength of 4 μm, respectively. Hereafter, we will refer to curve III, in which this constraint is obeyed, as the minimum loss curve, since the loss figures for the surface-like modes are not realistic in practice [15]. We plot the air-filling factor corresponding to the minimum loss as the red solid curve in Fig. 11(a). The black dashed curves represent the air-filling factor corresponding to the largest relative bandgap for each refractive index, which is the same as the black

#75986 - $15.00 USD Received 13 October 2006; revised 21 December 2006; accepted 22 December 2006

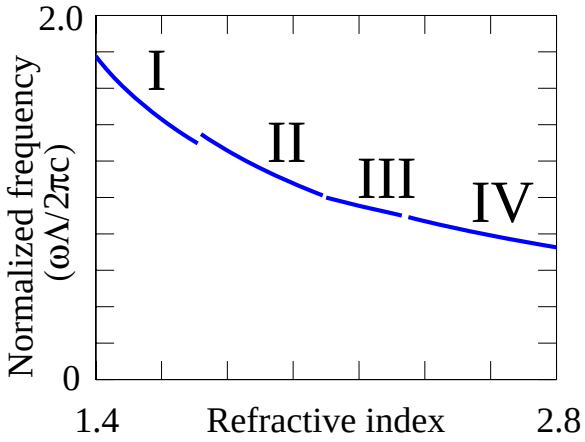

Fig. 12. The optimized normalized frequency corresponding to curves in Fig. 9 as a function of refractive index.

dashed curves in Fig. 2. The maximum difference between the air-filling factor corresponding to the maximum relative bandgap and the minimum loss is about 0.03. Figure 11(b) shows the relative bandgap when the air-filling factor corresponds to the dashed curve of Fig. 11(a), which is the maximum possible relative bandgap at each refractive index. The trends in Fig. 11(b) are the opposite of those in Fig. 9(a). When the relative bandgap decreases, the loss increases, and vice versa. The refractive index of 2.6, corresponding to the minimum loss, is higher than the refractive index of 2.2, corresponding to the maximum relative bandgap. The reason for this difference is that the higher refractive index contrast between the air and the glass helps to confine the mode in the center air hole. Hence, the refractive index corresponding to the minimum loss is somewhat higher.

Figure 12 shows the optimized normalized frequency corresponding to the curves in Fig. 9 as a function of refractive index. Note that the optimized normalized frequency decreases as the refractive index increases. The reason is that the field in a material with a higher refractive index will have a lower frequency than the field with a lower refractive index, assuming that the geometry and the propagation constant are fixed. The normalized frequency that we showed in Fig. 1 will decrease as the refractive index increases at a fixed propagation constant. Hence, the optimized normalized frequency decreases as the refractive index increases. The slight offset between curves I and II comes from the different bandgaps we discussed in section 2. The optimized normalized frequency shown in Fig. 12 will be useful in practical design of the air-guided PBGF.

Figure 13(a) shows the geometry and the corresponding mode intensity, normalized to its peak, for a 5-layer air-core PBGF using an refractive index of 2.6, an air-filling factor of 0.8 and a normalized frequency of 0.79 corresponding to the minimum shown in the curve IV in Fig. 9(a). The black circles represent the hole boundaries and the color contour plots represent the Poynting flux. Figure 13(b) shows the loss as a function of the number of air hole rings on a logarithmic scale with the same fiber parameter. Note that the loss is less than 1 dB/km with 9 air hole rings and a wavelength of 4 μm. This loss is lower than what can be obtained with 14 air hole rings with an air-filling factor of 0.9 for silica material with a refractive index of 1.45, as shown in Fig. 6 of Ref. 3. We have also carried out the optimization procedure with 6 and 7 air hole rings, and we find that the optimized air-filling factor and normalized frequency corresponding to minimum loss vary by 1% and 2%, respectively.

#75986 - $15.00 USD Received 13 October 2006; revised 21 December 2006; accepted 22 December 2006

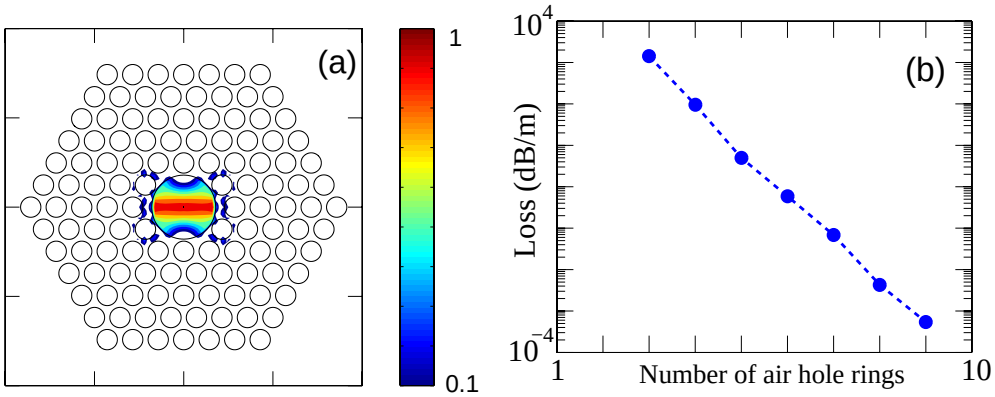

Fig. 13. (a) Geometry and corresponding normalized mode intensity for a 5-layer air-guided PBGF corresponding to the minima shown in the dashed curves in Fig. 9. Normalized mode intensity smaller than 0.1 is not shown. (b) The loss as a function of the number of air hole rings on a logarithmic scale with the same fiber parameter.

4. Conclusions

We show the relative bandgap when we vary the air-filling factor and the refractive index. We found that the relative bandgap has two maxima as a function of the air-filling factor and the refractive index, and we studied the mode characteristics at these two maxima. The difference between the air-filling factors for the maximum relative bandgap and the lowest loss is around 0.03, with a refractive index between 1.4 and 2.8. Thus, this work supports the assumption of Pottage, *et al.* [5] that the analysis of the unit-cell bandgap is a good indication of the optimal air-filling factor for air-core PBGF design. We also found that when the relative bandgap increases, the loss decreases, and vice versa. There exists a minimum loss in the high index region. The refractive index corresponding to this minimum loss is higher than the refractive index corresponding to the maximum relative bandgap, since a high index contrast helps to confine the mode. The optimal normalized frequency corresponding to minimum loss decreases as the refractive index increases.

Acknowledgments

This work is supported in part by the Naval Research Laboratory. We are grateful to B. Justus, L. B. Shaw, and J. S. Sanghera for suggesting this problem to us and for useful discussions.

#75986 - $15.00 USD Received 13 October 2006; revised 21 December 2006; accepted 22 December 2006